

Active Control of Rotor Aerodynamics and Geometry: Status, Methods, and Preliminary Results

Timothy J. McCoy^{*} and Dayton A. Griffin[†]
Global Energy Concepts, LLC, Kirkland, WA, 98034

The continued reduction in cost of energy (COE) of wind turbines will require contributions from technical advances in many areas. This research focuses on the combination of two areas: aerodynamics and controls. The goal of the overall study is to develop baseline estimates of the cost benefits available from the use of advanced control of wind turbine rotors including modification of rotor aerodynamics and geometry. This paper will present the current status, some methods used, and some preliminary results for load reduction.

The overall study explores two major categories of rotor aerodynamic modification. The first is devices or methods that can be used to actively alter the local aerodynamic properties of the rotor blade. The active aerodynamic devices being considered for the overall study include: flaps, slats, ailerons, active (MEM) tabs and vortex generators, “smart” materials such as shape memory alloys and piezoelectrics, and “morphing” structure technology for both large changes (i.e., camber modifications) and local shape changes (i.e., leading edge curvature). These devices would typically have response times on the order of, or faster than, a full-span, variable-pitch system. The control algorithms will employ linear state space methods that include individual blade pitch and multi-input, multi-output control of the selected aerodynamic devices. The second category of active rotor modifications is geometry control, based on variable-length blades.

These technologies are applied to a virtual turbine design, originally developed under the WindPACT program and up-rated for this study to a 90-m diameter, 2.5 MW, variable-speed, variable-pitch turbine. The approach will include simulations using MSC-ADAMS and detailed cost modeling based on the simulated loads.

The paper will present details of the aerodynamic and geometric designs developed to date, as well as the control strategy employed for both. Preliminary load results will be presented for the extendable blade design and for aerodynamic control using microtabs.

I. Introduction

As part of phase II of the National Renewable Energy Laboratory’s (NREL) Low Wind Speed Turbine (LWST) project, this paper is an interim status report on a study of the potential for active rotor geometry and aerodynamic controls to lower the cost of energy (COE). Two independent technologies are being studied: a variable-diameter rotor and advanced aerodynamic controls.

The concept for the variable-diameter rotor is to maximize energy capture in low winds while minimizing loads in high winds. The variable diameter will be achieved via extension and retraction of the tip section of the blade using an actively controlled mechanism. The advanced aerodynamic controls will be based on microtabs and other technologies to be identified using controls designed with multi-input, multi-output state space techniques. Both of these technologies will be modeled in the ADAMS general purpose dynamic simulation software coupled with the Aerodyn [1] routines available from NREL for aerodynamic loading calculations.

The effort to reduce wind energy COE requires that advances continue to be made in turbine architectural concepts, aerodynamics, and control (among other things). This research is intended to quantify the potential of the variable-diameter rotor and the aerodynamic controls to reduce COE. In both cases cost models will be applied that

^{*} Senior Engineer, 5729 Lakeview Drive, Suite 100, Kirkland, WA 98033.

[†] Engineering Project Manager, 5729 Lakeview Drive, Suite 100, Kirkland, WA 98033, AIAA Member.

are based on the performance and loads calculations. The cost benefits achievable with the candidate technologies will be compared to a baseline turbine that is of a size and architecture consistent with current commercial utility-scale wind turbines.

This paper will present selected interim methods and results, including aerodynamic, structural, and control design and loads results. The paper will focus on the variable-diameter rotor and aerodynamic control using microtabs.

II. BASELINE TURBINE

A baseline turbine design was chosen in order to make comparisons. The design was initially based on the work done in the WindPACT rotor study [2]. While the rotor study had its primary baseline rated at 1.5 MW, for this study a larger turbine was chosen since the technologies being examined are more likely to show benefit at a larger size. The following are the primary architectural details of the virtual design used for the baseline:

- 3-blade upwind, 90-m diameter, 2.5 MW, variable speed, pitch to feather
- 80-m tube tower, fiber glass reinforced polyester (FRP) blades, 3-stage gearbox with doubly fed generator
- Controls: torque speed curve to follow optimum TSR in low wind and a proportional-integral (PI) controller from rotor speed to collective pitch in high wind

The baseline blade aerodynamic design was developed using the PROPID inverse-design code [3], employing the S818 / S825 / S826 family of airfoils [4]. Following the methodology in Griffin [5], the blade structural design was developed using the ANSYS finite element code with NuMAD pre-processor [6] and the EBEAM code [7] for determining blade local mass and stiffness properties.

The blade spar was dimensioned at several spanwise locations, based on simulations of IEC load cases, and design properties for the fiber reinforced plastic (FRP) material assumed for the baseline blade structure. Considerations for the blade structural design included static and fatigue strength, as well as tip-tower clearance.

III. VARIABLE-DIAMETER ROTOR

A. Status

A first iteration of the variable-diameter rotor has been completed. This includes an aerodynamic trade study, a structural design, control design, and simulations in ADAMS. In characterizing this technology, the acronym “RBR” has been used to denote a “Retractable-Blade Rotor” and is used synonymously with “variable-diameter rotor.”

B. Methods

An aerodynamic trade study was conducted to determine an appropriate diameter range for the RBR rotor. The study assumed that the fixed inboard portion of the blade will have the same profile as the baseline blade. The extendable outboard section of the blade will be a constant chord, constant twist section sized to fit within the inboard section at the cut-off radius.

The performance calculations assumed that the maximum generator torque would be maintained at the same level as the baseline but that the rotor RPM could increase as the diameter decreased in high winds. This approach maintains the same maximum tip speed but allows the rated power to increase. Performance and annual energy results were calculated for several cut-off radii and several maximum lengths as indicated in Table 1. Based on the amount of predicted energy capture, and on assumptions regarding the feasibility of accommodating different blade tip lengths within the blade, configuration number 6 was chosen as the first candidate for simulation in ADAMS. This configuration is depicted graphically in Figure 1. The solid black outline shows the baseline blade chord dimensions. The blue line indicates the cut-line at 90% of the original radius, and the dashed lines indicate two possible locations for the extended RBR tip.

Table 1. Annual Energy (AEP) for Various Rotor Configurations

Configuration Number	Cut-off Radius (%R*)	Min. R (m)	Max. R (m)	Max Power (kW)	AEP (MWh)	Change in AEP (%)
0 (baseline)	N/A	45	45	2500	8,724	0.0%
1	95	45	50	2500	9,660	10.7%
2	95	45	55	2500	10,402	19.2%
3	90	45	50	2500	9,657	10.7%
4	90	45	55	2500	10,412	19.4%
5	90	42.75	50	2632	9,836	12.7%
6	90	42.75	55	2632	10,591	21.4%
7	85	45	50	2500	9,644	10.5%
8	85	45	55	2500	10,395	19.2%
9	85	40.5	50	2778	9,965	14.2%
10	85	40.5	55	2778	10,716	22.8%

* Percentage of original rotor radius **Selected candidate configuration**

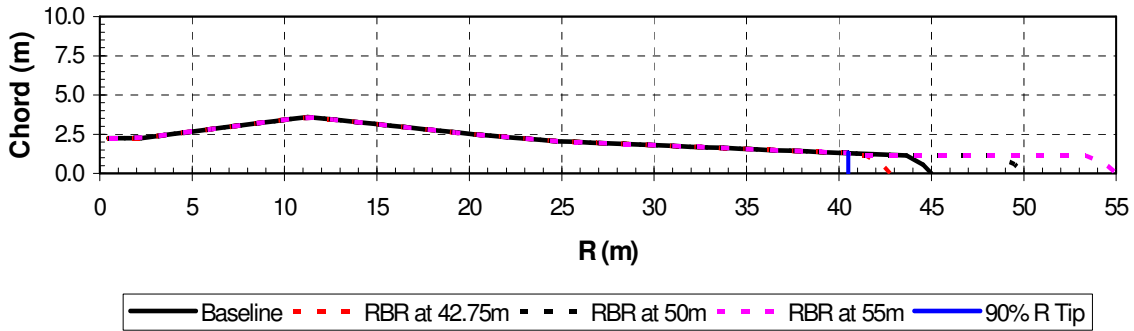


Figure 1. RBR Configuration Selected for Initial ADAMS Simulations

A rack and pinion with a servo motor was selected as the mechanism to drive the extendable/retractable blade tip. This mechanism has the desirable property that the motor inertia, when geared down to obtain low blade tip extension speeds, acts as a large inertial lag on the deployment of the tip. This allows a control algorithm design that can maintain a tight tolerance on the blade tip extension length without requiring very high gain.

The desired blade tip extension position is calculated using a linear function of wind speed. The wind speed input is filtered with a low pass filter that has a time constant of 30 seconds. The resulting demand is adjusted to limit the tip extension rate to a selected maximum. This demand is sent to a servo control algorithm. A control algorithm was designed for the servo motor using a simple state space model of the blade tip that includes the tip extension position and velocity along with an integral of the extension position error. The gains were calculated for a steady state linear quadratic regulator.

The standard turbine controls include a torque speed curve that is dependent on both rotor radius and RPM and a PI control for speed regulation with blade pitch.

One drawback to the ADAMS model is that the bearings for the tip mechanism are not modeled entirely accurately. ADAMS can not manage to track the changing contact locations for a linear bearing. As a result, the bearing reaction forces are not initially calculated correctly. These can be corrected in post processing.

Using the above described model, a selected set of IEC load cases was run in ADAMS. These cases included load cases 1a and 1b for normal operation in turbulence, extreme 50-year return wind speed with turbulence, and

most of the extreme deterministic gust cases. Many of these gust cases were run at a range of wind speeds to accommodate the range of diameters at which the turbine can operate.

IV. Preliminary Results

The resulting power curve for the variable-diameter rotor during normal operation in turbulence is shown in Figure 2. This is compared to the baseline power curve for the same set of turbulent simulations. Also shown is the mean radius versus wind speed. Note that the two curves come closest at a wind speed of 12 m/s and that the power output of the variable-diameter rotor is higher even though the radius is less than the 45-m radius of the baseline rotor. This is because the rotor speed and power output are allowed to increase while tip speed and torque remain at the baseline levels. An example time trace of rotor radius versus wind speed is shown in Figure 3.

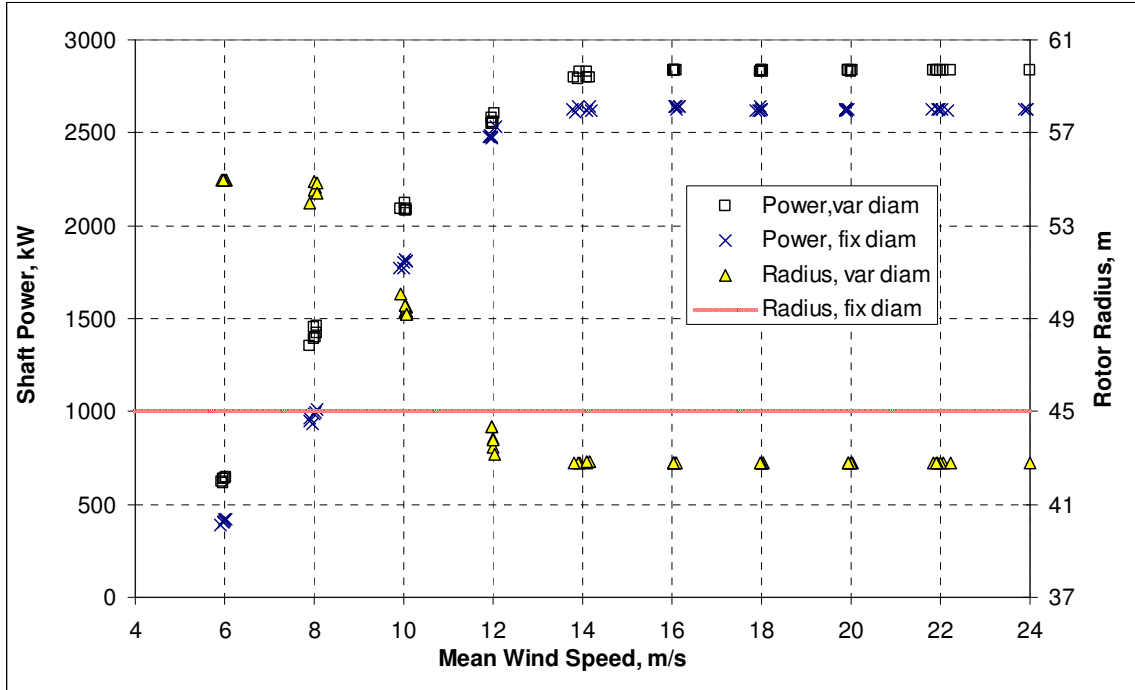


Figure 2. Comparison of power performance: variable-diameter rotor versus fixed diameter baseline

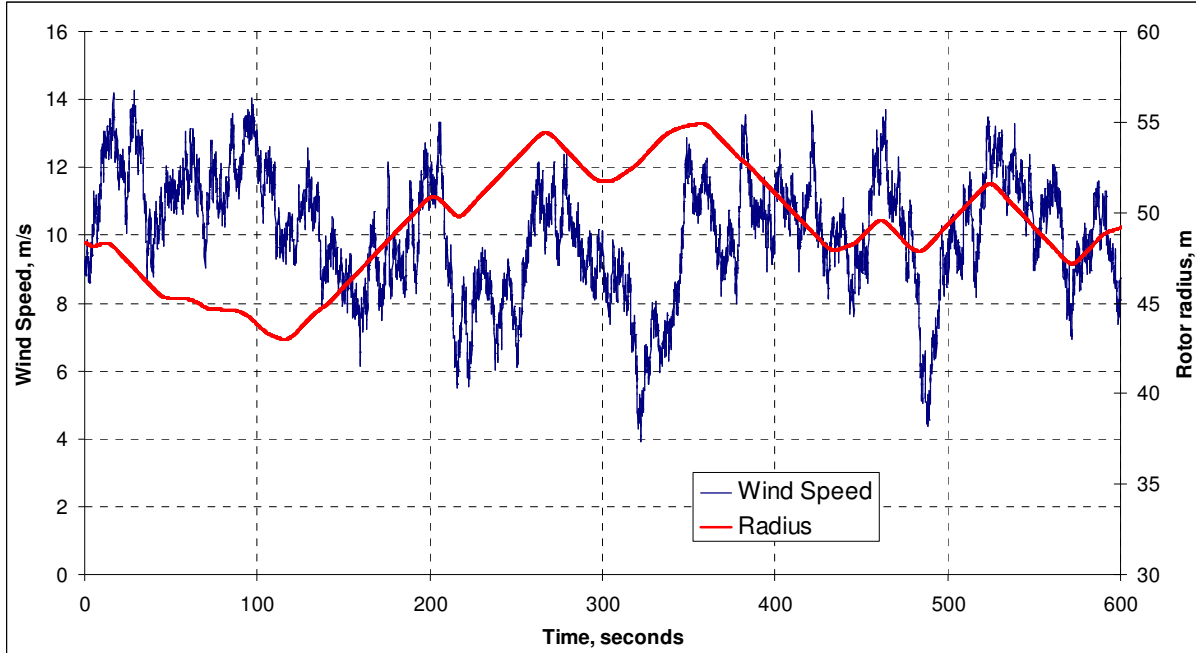


Figure 3. Wind speed and rotor radius for operation in turbulence at 10 m/s

As expected, both peak and fatigue loads have gone up for the variable-diameter rotor as compared to the baseline. This is due to the increase in the length of the blade in lower wind speeds that result in more overall rotor thrust and higher blade root and tower base bending loads. Use of more advanced control strategies may be able to trim these load increases a bit relative to the baseline PI control. Table 2 compares the peaks for a select set of loads. Table 3 compares fatigue equivalent loads.

Table 2. Comparison of Peak Loads Between Variable Diameter and Baseline Turbines

Load Component	Baseline		Variable Diam		% change
	Maximum	Load Case	Maximum	Load Case	
Root Edge bending, kNm	2,350	ECD_R	2,580	ECD 10m/s	9.8
Root Flap bending, kNm	5,010	ECD_R	5,590	PP 22m/s	11.6
Main shaft bending, kNm	3,760	ECD_R	4,350	ECD 10m/s	15.7
Main shaft torque, kNm	1,780	PP 24m/s	1,830	PP 24m/s	2.8
Tower top roll, kNm	2,080	PP 24m/s	2,120	PP 24m/s	1.9
Tower top tilt, kNm	-6,070	ECD_R	-6,600	ECD 10m/s	8.7
Tower top yaw, kNm	2,840	PP 24m/s	3,490	ECD 8m/s	22.9
Tower base, kNm	49,670	EWM 1 year	52,260	EWM 1 year	5.2
Blade Tip Deflection, m	5.06	ECD_R	7.98	ECD 8m/s	57.7

Table 3. Comparison of Fatigue Equivalent Loads Between Variable Diameter and Baseline Turbines*

Load Component	SN slope	Baseline	Var Diam	% change
Root Edge bending, kNm	15	2594.0	3084.5	18.9
Root Flap bending, kNm	15	2756.9	2945.6	6.8
Main shaft bending, kNm	8	1,950.0	2,107.5	8.1
Main shaft torque, kNm	12	717.7	747.7	4.2
Tower top roll, kNm	8	513.9	531.2	3.4
Tower top tilt, kNm	8	1,623.6	1758.1	8.3
Tower top yaw, kNm	8	1,621.7	1681.0	3.7
Tower base, kNm	4	6,283.5	7,090.5	12.8

* $Neq = 20 \text{ years/lifetime} * 8760 \text{ hrs/yr} * 3600 \text{ cycles/hr} = 6.3E8 \text{ cycles/lifetime}$

V. Conclusions and Future Work

Continued investigation of the variable-diameter rotor analysis will depend on comments from our research partner. Most likely this will include changing the extendable tip length to determine the optimum.

While the detailed design of the mechanism for blade extension and retraction will be a challenge, one issue that was made clear during this research is that designing and building the basic blade structure will be an equal challenge. The efficiency of the blade structure is very difficult to maintain given an initial blade design consistent with a typical 2.5 MW blade. We discovered that significant amounts of carbon fiber were required to attain both the strength and stiffness needed to support the extension segment and the outboard portion of the fixed part of the blade.

VI. ACTIVE AERODYNAMIC CONTROLS

A. Status

Use of active aerodynamic controls to reduce dynamic loads makes up the second phase of this research. Most of the effort to date has been development of the aerodynamic properties, building the ADAMS model, understanding and modifying the aerodynamics subroutines, and developing control routines and strategies. Also completed are some preliminary control designs and loads results.

B. Methods

The active aerodynamic devices considered for this study included flaps, slats, ailerons, active (MEM) tabs and vortex generators, “smart” materials such as shape memory alloys and piezoelectrics, and “morphing” structure technology for both large changes (i.e., camber modifications) and local shape changes (i.e., leading edge curvature). These devices would typically have response times on the order of, or faster than, a full-span, variable-pitch system. Figure 4 depicts some examples of aerodynamic control devices considered for modeling in this study.

The aerodynamic device chosen for initial work is the micro tab being studied by vanDam [8]. The aerodynamic properties associated with this device for use in the controls development and loads simulations were developed essentially by hand using the published work as a reference. Plots of the estimated lift and drag effects on the S825 airfoil are shown in Figure 5.

Several idealized and simplifying assumptions were made as follows:

- The aerodynamic effects that result from device deployment are very fast (no time lag).
- The devices can be deployed continuously from one end of their range to the other.
- The devices deploy in both a positive and negative fashion with resulting approximately symmetrical aerodynamic effects.

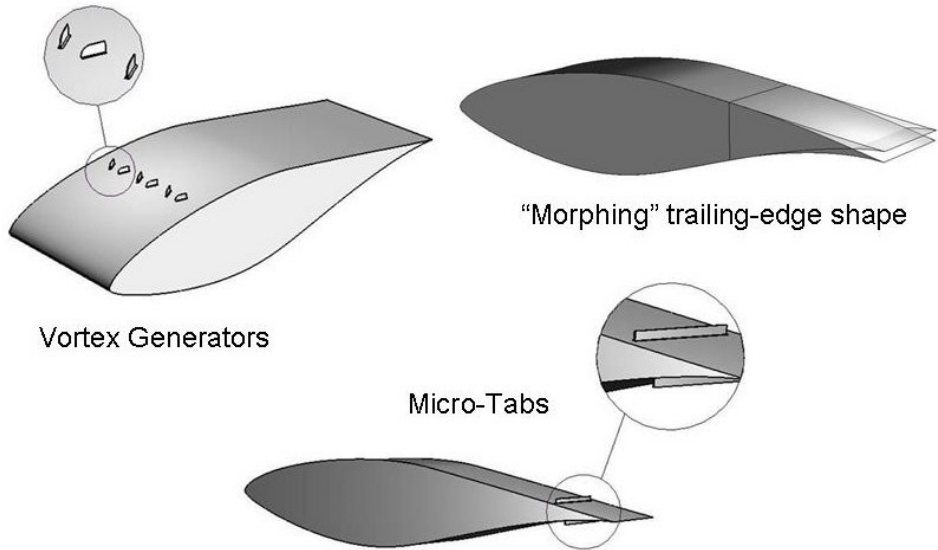


Figure 4. Example Candidate Technologies for Active Aerodynamic Control

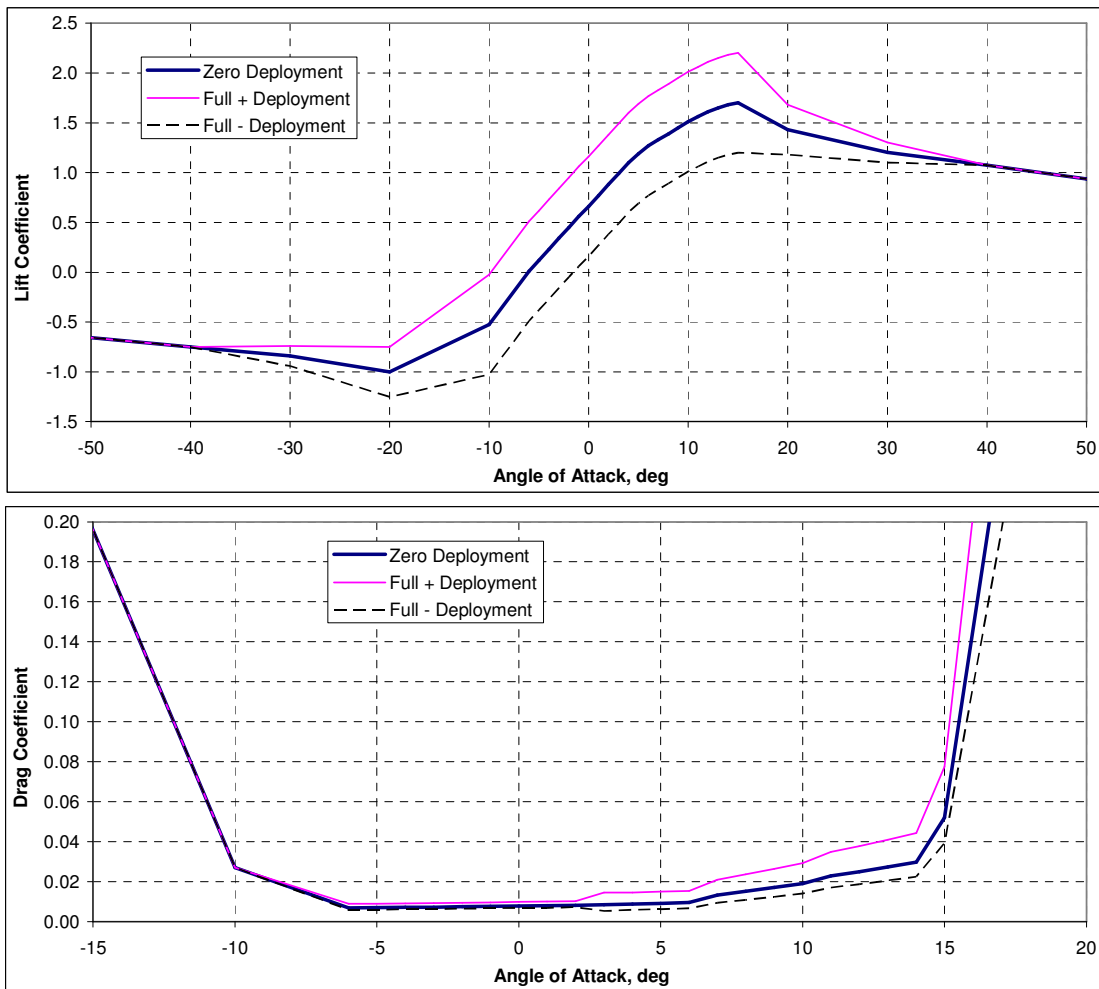


Figure 5. Lift and drag coefficients for the S825 airfoil with micro tab effects

These assumptions allow the use of linear state space control theory for gain selection. One significant limitation of these devices is that they have a limited range of deployment. Unlike blade pitch which can traverse a wide range of angle and aerodynamic effects, micro tabs have a limited deployment range. The control design is tuned to avoid reaching these limits.

In order to develop linear models of the turbine for use with control design, aerodynamic derivatives of controls and wind disturbances were developed numerically using ADAMS and the Aerodyn subroutines. The micro tab effects were lumped into three regions of the blade: inboard, midspan, and outboard. Deployment of the tabs is done together in each of these three regions. Deployment direction is either + or - for, respectively, increased or decreased lift and drag as indicated in Figure 5. Plots of the thrust and torque changes for full micro tab deployment in each of these three regions are shown in Figure 6 versus wind speed.

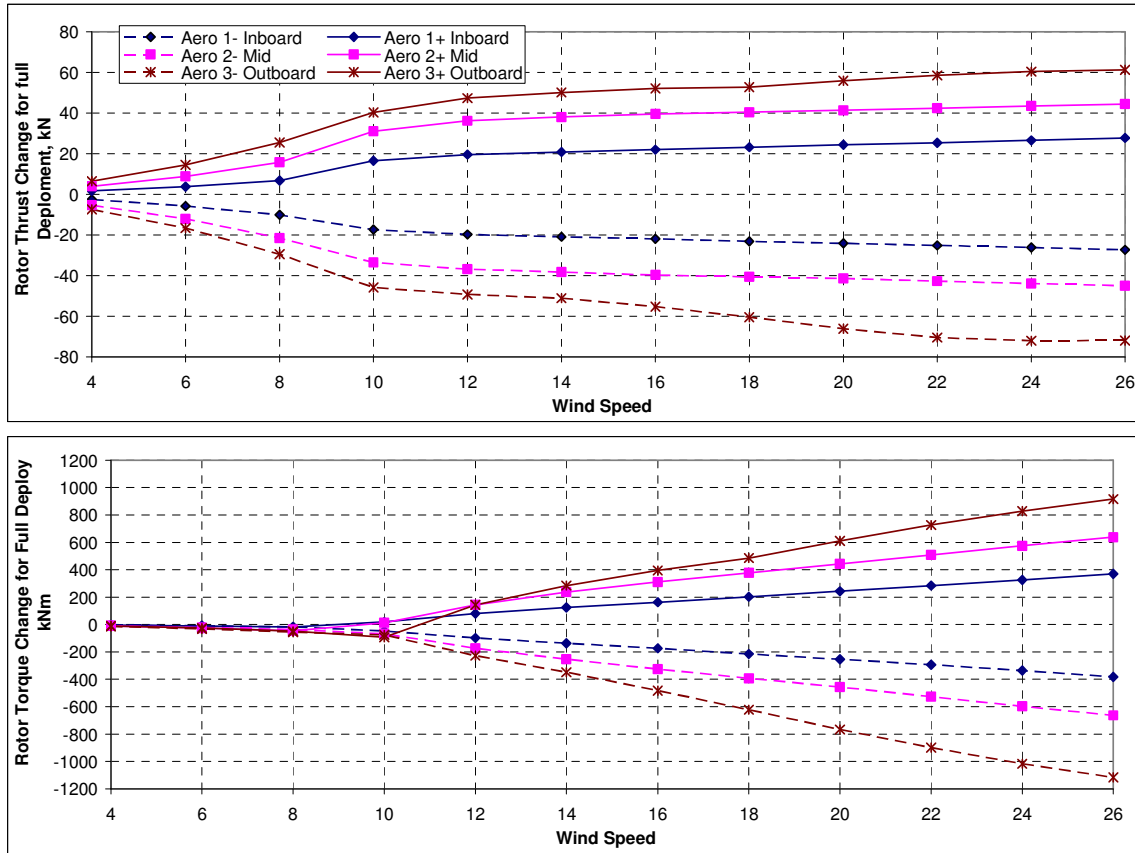


Figure 6. Aerodynamic derivatives for aerodynamic controls around stable operating points (+/- indicates deployment for increased or decreased lift respectively)

The aerodynamic derivatives are used in the linearization process developed by McCoy [9] for use with the ADAMS structural model. The linearization methodology also transforms the rotor periodicity into a time invariant model entirely expressed in the fixed frame. The control design is based in the fixed frame but is transformed into appropriate control behavior on the rotor via the azimuth angle and a multi-blade transformation as described in Coleman [10]. This method allows for independent blade pitch (IBP) and independent blade (IB) aero control.

The resulting linear model is reduced to the primary modes and transformed into physical states. The system poles, corresponding to the frequency and damping of the selected aeroelastic modes for the baseline rotor, are shown in Figure 7 for the linearized model about a stable operating point at 20 m/s. The control design assumes full state knowledge and uses a steady state linear quadratic regulator (LQR) to select the gains.

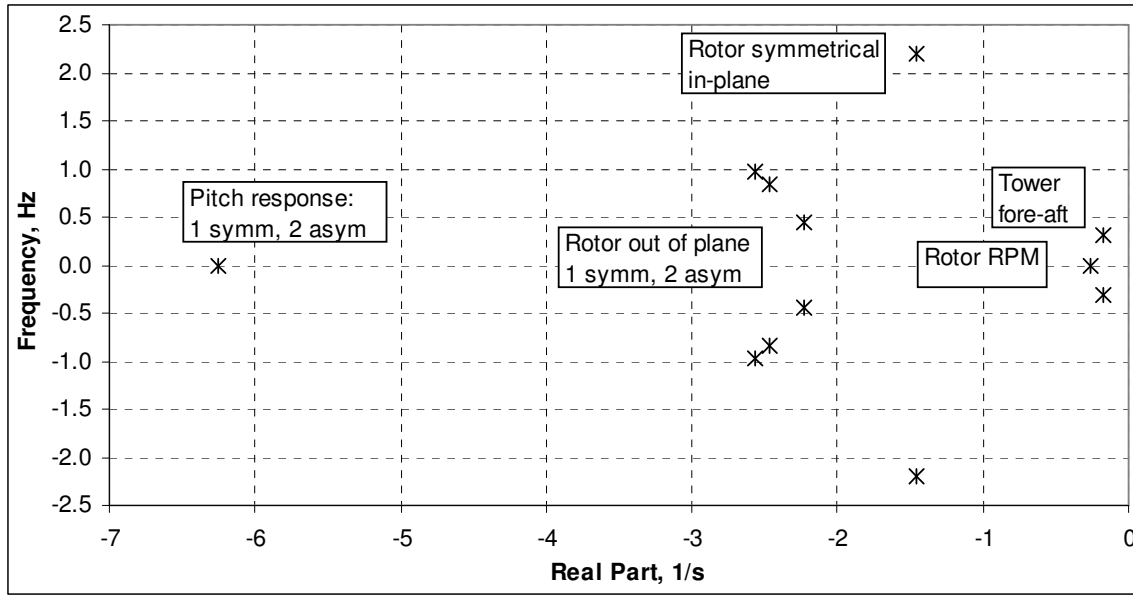


Figure 7. Structural modes of linearized model, including coupled aero effects

The process of designing a control structure for the operating range of the turbine and tuning the gains by selecting LQR weightings proved to be challenging. Several issues arose that had to be addressed in the design of the overall controller structure. These included:

- Saturation of the micro tab controls. Unlike blade pitch the micro tabs have a finite range of deployment. The control design had to avoid demanding both excess deployment and drift. As wind conditions varied, the demand on the micro tabs tended to drift outside their physical range. The solution to this problem has been to include an integral of the micro tab demand in the state model and regulate it to achieve a mean demand of zero deployment.
- Transition from the low wind region that primarily uses torque for speed control to a high wind region that uses symmetric blade pitch for speed control. Switching logic was developed that detected the requirement for a transition and implemented it, including resetting a number of integral states. This switching is used to transition between gain sets also.

The following provides specific details regarding the control architecture and design:

- The turbine operation is broken into distinct regions with a unique LQR state space control design for each region:
 1. RegionIIA – From cut-in up to about 10 m/s, the generator torque is calculated as gain times RPM². The mean pitch is allowed to vary but held to a nominal set point on average by an integrator. Independent blade and aero controls are all active to provide fatigue load reduction. Exit when RPM reaches max set point.
 2. RegionIIB – Rotor speed must be regulated to its maximum nominal value. The blade pitch and aero control is the same as region IIA and has the sole purpose of load reduction. The generator torque control is used to regulate the RPM with a state-space (linear quadratic regulator gain selection) controller that includes gains on rotor RPM, tower states, and measured wind speed. Exit when the generator torque reaches its maximum set point.
 3. RegionIIIA – Wind speed up to 16 m/s. The generator torque is held at its maximum set point. Independent blade pitch and aero controls are used for RPM and load control via a state-space algorithm.
 4. RegionIIIB – Wind speed from 16 m/s up to cut-out. Similar to regionIIIA with a new set of state space gains.

- When the controller changes regions, the integrals are reset by inverting the gain sub matrix for the integral states: $X_I = \text{inv}(K_I) * (U_0 - U - K * X)$

VII. Preliminary Results

To check the efficacy of the controls and as an example, the effect of independent blade pitch and independent blade aero control is shown in Figure 8 compared to the baseline PI control. In this example the wind speed is held at 14 m/s but the logarithmic wind shear exponent is stepped from $\alpha = 0.0$ to $\alpha = 0.2$ at time = 100 seconds. With a PI controller the blade tip deflections show a clear variation at once per rev. The blade pitch and RPM are only affected imperceptibly.

However with independent blade pitch the once per rev variation is reduced over time. The tip deflection variation could be reduced more quickly; however, this would require more pitch action at the expense of other response such as the tower. The micro tab aero controls can also be used to eliminate the once per rev blade tip variations. Note that the variation is reduced much more quickly.

A set of IEC load case runs was completed for a preliminary control design. Table 4 and Table 5 show the results from these simulations for peak and fatigue equivalent loads. A comparison of power output in low winds showed that the use of these aerodynamic controls had minimal effect on power output compared to the PI controlled baseline. It has been observed that aggressive variation of pitch and aero control in lower wind speeds does affect average power output; however, the controls would typically be tuned to avoid this.

VIII. Conclusions and Future Work

In general it appears that use of aerodynamic controls can improve the turbine peak and fatigue loading. The primary lessons learned to date on this project are that the limitations of linear control theory require that any aerodynamic device behave in a reasonably linear manner. For example, actuator saturation must be avoided. The challenge will be to find the most effective control approach to optimize the use of specific devices. Future work that is outside the scope of this investigation would look at increasing rotor diameter in order to increase annual energy output for the same level of fatigue loading as the baseline.

Effort on the design of the aerodynamic controls will continue in the following areas:

- Improve the control design for the micro tabs
- Repeat the exercise with alternate aerodynamic devices
- Remove some of the assumptions, such as the instantaneous response of the aero devices

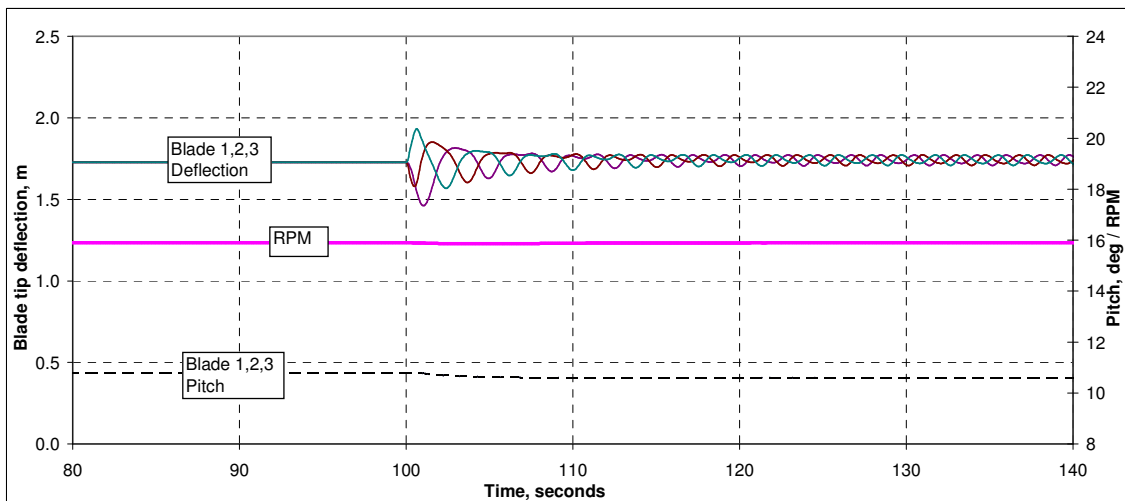
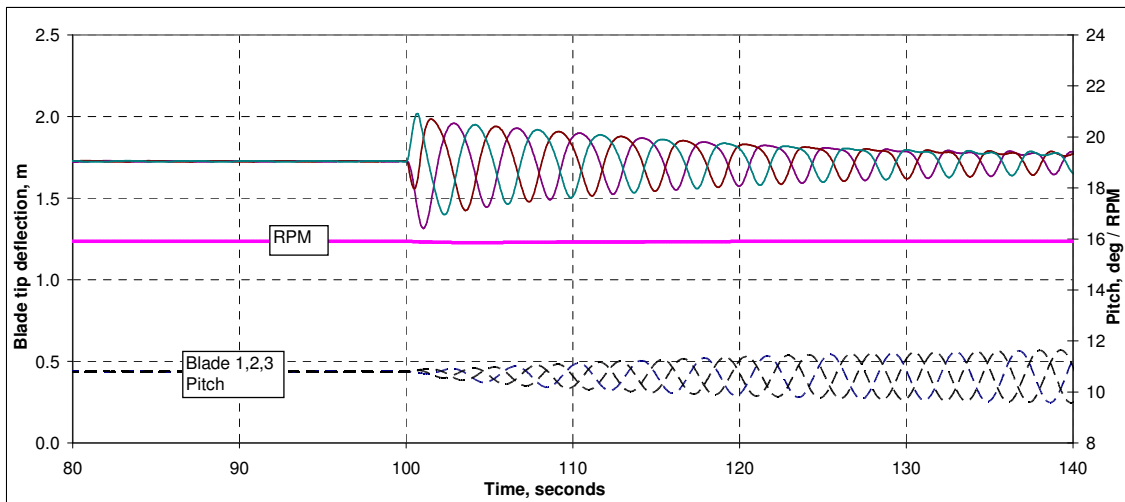
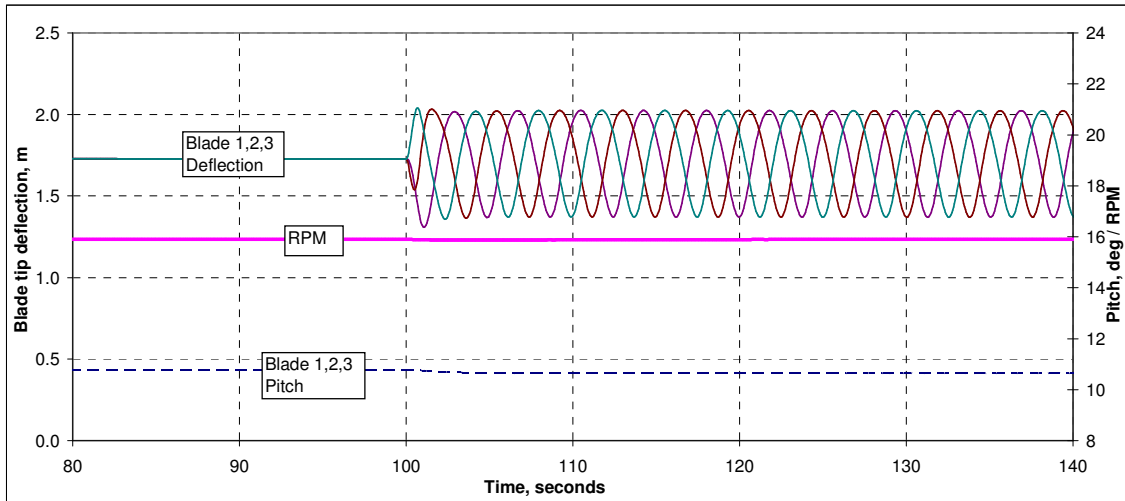


Figure 8. Comparison of load reduction using (from top to bottom) the PI, IBP, and IBAero controls for a step change in wind shear at 14 m/s.

Table 4. Comparison of Peak Loads Between Aero Controls and Baseline Turbines

Load Component	Baseline		Aero Controls		% change
	Maximum	Load Case	Maximum	Load Case	
Root Edge bending, kNm	2,350	ECD_R	2,690	ECD_R	14.5
Root Flap bending, kNm	5,010	ECD_R	4,730	ECD_R	-5.6
Main shaft bending, kNm	3,760	ECD_R	3,420	ECD_R	-9.0
Main shaft torque, kNm	1,780	PP 24m/s	1,660	PP 22m/s	-6.7
Tower top roll, kNm	2,080	PP 24m/s	1,970	PP 24m/s	-5.3
Tower top tilt, kNm	-6,070	ECD_R	-5,760	ECD_R	-5.1
Tower top yaw, kNm	2,840	PP 24m/s	2,790	PP 24m/s	-1.8
Tower base, kNm	49,670	EWM 1 year	49,670	EWM 1 year	0.0
Blade Tip Deflection, m	5.06	ECD_R	4.67	ECD_R	-7.7

Table 5. Comparison of Fatigue Equivalent Loads Between Aero Controls and Baseline Turbines

Load Component	SN slope	Baseline	Aero Controls	% change
Root Edge bending, kNm	15	2594.0	2543.5	-1.9
Root Flap bending, kNm	15	2756.9	2166.7	-21.4
Main shaft bending, kNm	8	1,950.0	1446.5	-25.8
Main shaft torque, kNm	12	717.7	729.9	1.7
Tower top roll, kNm	8	513.9	510.3	-0.7
Tower top tilt, kNm	8	1,623.6	1363.3	-16.0
Tower top yaw, kNm	8	1,621.7	1387.2	-14.5
Tower base, kNm	4	6,283.5	5342.0	-15.0

* Neq = 20 years/lifetime*8760 hrs/yr*3600cycles/hr = 6.3E8 cycles/lifetime

IX. Acknowledgements

This work was supported by the National Renewable Energy Laboratory under subcontract YAM-4-33200-08.

X. References

1. Windward Engineering, *Aerodyn User's Guide, Version 12.50*, December 24, 2002.
2. Malcolm, D.J., and Hansen, A.C., *WindPACT Turbine Rotor Design Study*, NREL/SR-500-32495, National Renewable Energy Laboratory, August 2002.
3. Selig, M.S.; and Tangler, J.L., *A Multipoint Inverse Design Method for Horizontal Axis Wind Turbines*, Presented at the AWEA Windpower '94 Conference, Minneapolis, MN, May 1994.
4. Tangler, J.L.; and Somers, D.M., *NREL Airfoil Families for HAWTs*, Presented at the American Wind Energy Association Windpower '95 Conference, Washington, DC, March 1995.
5. Griffin, D.A., *Blade System Design Studies Volume II: Preliminary Blade Designs and Recommended Test Matrix*, SAND2004-0073, Sandia National Laboratories, June 2004.
6. Laird, D.L., *2001: A Numerical Manufacturing and Design Tool Odyssey*, Proceedings of AIAA/ASME Wind Energy Symposium. Reno, Nevada, January 2001.
7. Malcolm, D.J. and Laird, D.L., *Modeling of Blades as Equivalent Beams for Aeroelastic Analysis*, AIAA-2003-0870, American Institute of Aeronautics and Astronautics, Reno, Nevada, January 2003.
8. vanDam, C.P et. al., *Computational and Experimental Investigation into the Effectiveness of a Microtab Aerodynamic Load Control System*, Sandia National Laboratories, August, 2004, DRAFT
9. McCoy, T.J., *Wind Turbine ADAMS Model Linearization Including Rotational and Aerodynamic Effects*, American Institute of Aeronautics and Astronautics, Reno, Nevada January, 2004.
10. Coleman, R.P. and Feingold, A.M., *Theory of Self-Excited Mechanical Oscillations of Helicopter Rotors with Hinged Blades*, NACA Technical Report TR 1351, 1958.